CIMAC CONGRESS 25
ZURICH, MAY 19 – 23, 2025

2025 | 450

Ammonia cracking: enabler for ammonia engines in power generation applications

New Engine Concepts & Systems

Nicole Wermuth, Graz University of Technology

Maximilian Malin, LEC GmbH
Andreas Wimmer, Graz University of Technology
Florian Rümmele, Fraunhofer Institute for Solar Energy Systems ISE
Robert Szolak, Fraunhofer Institute for Solar Energy Systems ISE

ABSTRACT

The global transition from an energy system based on fossil fuels to one based on renewable energy will also increase the need for dispatchable power generation in order to compensate the fluctuations from wind and solar electricity production. As a carbon-free energy carrier that has significant advantages in terms of storage and transportation, ammonia use for power generation is currently considered by many engine OEMs and power producers. The ignition and combustion properties of ammonia, however, are not beneficial compared with state-of-the-art fuels. Especially the low laminar flame speed and the high minimum ignition energy in comparison with other e-fuel options are considered to be detrimental for use in an internal combustion engine. These challenges can be overcome with the admixing of a more reactive fuel, such as hydrogen or diesel fuel. In order to avoid the need to store a second fuel, it was proposed to use ammonia decomposition upstream the engine to produce a hydrogen-rich gas that can act as an ignition enhancer.

This article describes the development of an ammonia cracker that uses an electrically supported catalyst carrier, a proven technology for thermochemical hydrogen production. An assessment of the most favorable engine combustion concepts based on experimental results on a single-cylinder research engine provides the requirements for the ammonia cracker, in particular the mass flow rate for different load conditions and the required pressure level. Further requirements such as quick start capability and modular design are considered in the overall concept and the system layout. Experimental results and simulation of reaction and flow conditions are presented together with an outlook on overall cracker performance.

1 INTRODUCTION

The global carbon dioxide (CO_2) concentration in the atmosphere is continuously rising by 2 – 3 ppm per year and has already passed the 420-ppm mark in the last couple of years [1]. The emission of CO_2 and other gases with a high global warming potential (GWP) must be reduced quickly and will likely have to be combined with technologies to actively remove CO_2 from the atmosphere to limit global warming to 1.5 K above pre-industrial levels [2]. The global transition from a fossil fuel-based energy system to a low or carbon-neutral energy system that is built on renewable energy sources (RES) such as wind power and photovoltaics is going to be crucial. One of the key challenges of the energy transition is the necessity to store large amounts of energy. Storage in the form of chemicals or e-fuels, e.g., ammonia or methanol, offers large storage capacities over long periods of time and even seasonal storage. The efficiency of the production process and the energy demand of the carbon capturing are reflected in the fuel costs, that are currently significantly higher for e-fuels than for fossil fuels (Figure *1*). Projections by the International Renewable Energy Agency [3], however, show a substantial decrease of e-fuel cost by 2050. To balance the electricity demand and the volatile supply by RES flexible and dispatchable back-up solution to ensure a stable and steady energy supply are required. Internal combustion engines in combined heat and power plants provide renewable electricity with centralized or distributed power generation.

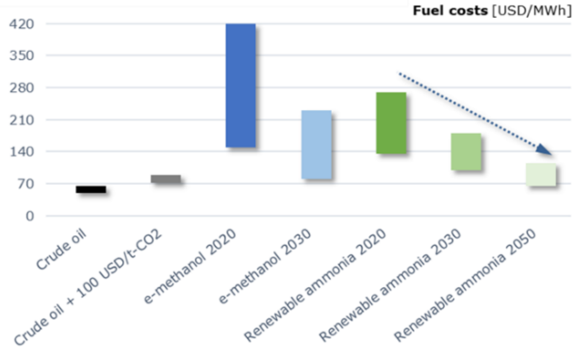

Figure 1: Current cost and cost projections for fossil fuels and e-fuels (based on [3])

1.1 Ammonia for power generation

The ignition and combustion properties of ammonia are not beneficial compared to state-of-the-art fuels. Especially the low laminar flame speed and the high minimum ignition energy in comparison to methane and hydrogen (Table *1*) was often considered to be detrimental for use in an internal combustion engine.

Table 1: Fuel properties of methane, ammonia and hydrogen

	Methane	Ammonia	Hydrogen
Lower heating value [kJ/kg]	50,013	18,720	120,000
Laminar flame speed [m/s]	0.38	0.07	3.50
Min. ignition energy [mJ]	0.290	8.000	0.017
Autoignition temperature [K]	868	930	858

Various fuel admission and ignition concepts are feasible for different engine applications (Figure *2*). To overcome the challenges posed by the ammonia properties the admixing of a more reactive fuel is useful [4]. For marine applications where redundancy requirements are usually adhered to by providing diesel engine operation capability, diesel fuel is used in ongoing research as the reactive fuel component. For spark ignition applications hydrogen is a suitable high reactivity fuel that can be produced via ammonia cracking.

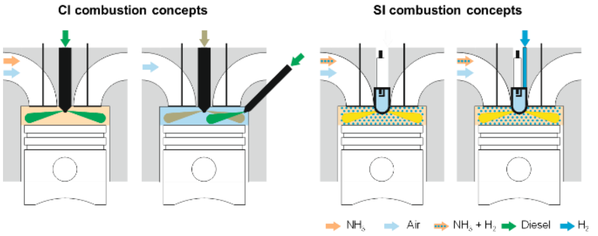

Figure 2: Combustion concepts for compression ignition engines (left) and spark ignition engines (right)

Ammonia dehydrogenation or cracking is a chemical process that involves the thermal decomposition of ammonia into its main components, molecular nitrogen (N_2) and molecular hydrogen (H_2). The simplified reaction equation can be described as follows [5]:

$$2\ NH_{3(g)} \rightleftharpoons 3\ H_{2(g)} + N_{2(g)} \qquad \Delta_R H = +\ 45.9\ \text{kJ/mol}_{NH_3} \tag{1}$$

The reaction is favored at high temperatures and low pressures, considering that it is endothermic and occurs with an increase in the number of moles. This endothermic reaction requires energy to break the chemical bond within ammonia and temperatures above 180 °C to be thermodynamically feasible [6]. At ambient pressure the equilibrium conversion of ammonia reaches values above 99 % at 400 °C while elevated pressures require even higher temperatures to achieve sufficiently high conversion rates. The high energy demand is one of the main concerns about the overall process economics. Therefore, it is advantageous to convert only a part of the ammonia into hydrogen and to adapt it to the engine operation.

Ammonia decomposition can be accomplished via thermal cracking, catalytic cracking or steam cracking [7]. Thermal cracking of ammonia is performed at temperatures around 1000 °C without the presence of a catalyst. Catalysts can improve the rate of ammonia decomposition and reduce the temperature and pressure required for this process. Apart from decreasing energy consumption, this can also extend the lifetime of the equipment and decrease production costs. In steam cracking ammonia is combined with steam and subjected to elevated temperatures in the presence of a catalyst.

Typical catalysts include noble metals such as platinum (Pt), ruthenium (Ru) and palladium (Pd), as well as metal oxides such as iron oxide (Fe_2O_3) and aluminum oxide (Al_2O_3). Catalysts are often based on metal nanoparticles supported on high surface area metal oxide and modified by different types of promoters [8], usually alkaline [9]. Fe-based catalysts and Fe–Co alloy-based ammonia cracking catalysts are typically bulk-based catalysts due to the relatively low cost of iron.

Ni-based catalysts are proven to be effective at high temperatures and show a high technology readiness level while Co–Fe based or Fe-based catalysts can work at medium temperatures [8]. Ru-based catalysts offer the advantage of working at low temperatures but are often considered uneconomical for the industrial scale due to the high cost. While catalysts can significantly improve the ammonia cracking process, they can also present challenges, such as poisoning or deterioration over time due to the accumulation of impurities or adverse operating conditions. The choice of catalyst can influence the selectivity of the products obtained with some catalysts favoring the production of hydrogen over nitrogen, while others may enhance the selectivity towards nitrogen.

The catalytic cracking of ammonia starts with the adsorption of ammonia on the active sites, followed by a successive N-H bond scission, and then formation of N-N and H-H bonds for nitrogen and hydrogen recombination, respectively. In [10] it was found that the rate-determining step (RDS) of the ammonia decomposition changes with the operating temperature. At low temperatures (300–500 °C), the RDS is $N*$ recombination, while at higher temperatures the RDS switches to the first $N-H$ cleavage. In [11] it was reported that the RDS of NH_3 decomposition is the cleavage of N–H bond for noble metals and the desorption of N_2 for non-noble metals.

Large-scale reforming reactors predominantly operate in allothermal mode, meaning that the heat for the endothermic reforming process is generated by a burner unit. The heat supply to the reaction zone occurs through the wall. Those processes are suitable for stationary applications and limited in terms of dynamics and start-up times. The reactor limitation is the heat transfer rather than the kinetics of the reforming reaction.

For dynamic applications, such as in internal combustion engines, autothermal heat supply is suitable. The heat generation occurs directly in the reaction zone through catalytic partial oxidation of the feedstock. In ammonia reforming, therefore a portion of the ammonia is oxidized to provide the energy for the endothermal reaction (see Equation 1).[12] For this operating mode the choice of reactor and the catalyst selection needs to consider the risk of H_2O adsorption on the active sites, which may compete with NH_3 and O_2, hindering the hydrogen production [8] as well as the process heat management, ensuring that the heat generated in the combustion section is effectively transferred to the reforming section. Kim et al. [13] found that fuel-rich mixtures with an equivalence ratio of 1.25 are favored for reduced nitrogen oxide (NO_X) formation.

Furthermore, the required heat can be provided electrically. The benefits of electrical heating are faster responses to demand changes, uniform heating, and pollutant-free operation. In one application the cracker could be fully operated within 10 minutes from room temperature and achieved 9.5 kWh electrical power consumption per kilogram of produced hydrogen.[6] A drawback of the electrical heater is that heat integration between the reactor and a potential H_2 purification step is not feasible, limiting the energy efficiency of the process. Induction is another option, but it requires special non-conductive wall materials, and the heat is provided from the outside.

Additional to different heating concepts membrane reactor concepts are investigated in literature, in which the chemical reaction and separation of H_2 through permeation by a palladium membrane are performed in a single step. This type of reactor is particularly suitable for applications where highly purified hydrogen streams are crucial, such as for proton-exchange membrane (PEM) fuel cells. Internal combustion engines are more tolerant to fuel impurities than PEM fuels cells. Therefore, the high purity hydrogen that a membrane reactor can provide is not required on engine applications.

In recent years ammonia crackers development are specifically designed for engine-based applications which means that only small fractions of ammonia need to be decomposed to hydrogen to serve as ignition and combustion promoter and where there are little to none purity requirements for the produced hydrogen [14][15].

In this article, a new technology concept is investigated and described in more detail in Chapter 3. The study focuses on conversion rates, power demand, and achievable gas hourly space velocities (GHSV). Experimental investigations of ammonia combustion concepts on a single cylinder research engine are used to derive the hydrogen demand profiles for the ammonia cracker. Based on these profiles and the requirements for fast start-up capability, modularity and high transient response the cracker layout is developed using theoretical considerations and thermodynamic simulations. Experimental investigations on a small-scale cracking unit are conducted to assess the performance potential and allow the specification for a scaled-up cracker unit for integration into a multi-cylinder engine (MCE) system.

2 SPARK IGNITION AMMONIA ENGINE COMBUSTION

Spark ignition (SI) combustion concepts for ammonia engines predominantly use external mixture formation of ammonia and air and employ hydrogen in various quantities as an ignition promoter. The hydrogen is usually mixed with the ammonia-air mixture in the intake manifold. Spark ignition concepts span the range from direct ignition concepts with a centrally mounted spark plug in the main combustion chamber to prechamber ignition concepts with different scavenging variants.

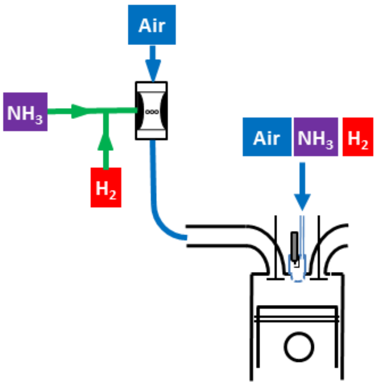

Figure 3: Schematic of the NH_3 combustion concept

The prechamber concept enables mixture stratification with a fuel-rich mixture in the prechamber or additional hydrogen supply directly into the prechamber to enhance the ignition conditions at the spark plug location. Adding hydrogen directly to the prechamber instead of the intake mixture might enable an overall reduction of the required hydrogen fuel quantity. The combustion concept employed in this paper is using external mixture formation and a scavenged prechamber. The concept is shown schematically in Figure *3*.

2.1 Experimental test set-up

The experimental investigations were carried out on a high-speed 4-stroke single cylinder research engine Figure *4*.

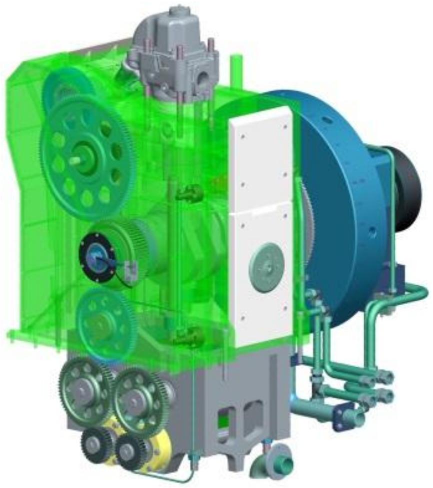

Figure 4: Singe-cylinder research engine

For the present investigation the single cylinder research engine (SCE) is equipped with a centrally located pre-chamber and a shallow piston bowl designed for a compression ratio slightly increased compared to a typical gas engine. The engine features a single camshaft with early intake valve closing (IVC) before bottom dead center (BDC). Further details of the engine configuration can be found in Table *2*.

Table 2: SCE technical specifications

General information	
Rated speed	1500 min^{-1}
Displacement	≈ 3 dm^3
Valve timing	Miller valve timing
Number of intake and exhaust valves	2/2
Charge air	Provided by external compressors with up to 10 bar boost pressure
Hydrogen supply	Venturi mixer upstream engine cylinder
Ammonia supply	Venturi mixer upstream engine cylinder
Ignition system	Supported via pre-chamber

All engine fluids including cooling water, lubricating oil, fuel gas and charge air temperature are controlled to ensure well-defined and reproducible testing conditions. In lieu of a turbocharger, an air compressor upstream of the engine and a flap in the engine exhaust system are used to adjust intake and exhaust manifold pressures. The test bed is equipped with crank angle (CA) and time-based measurement technology for all relevant parameters. Piezoelectric pressure sensors were used for pre-chamber, main chamber and intake and exhaust port to investigate the thermodynamic process during the combustion. In order to acquire highly reliable and reproducible exhaust gas measurements, an IAG FTIR system was used to cover the whole range of exhaust gas components of interest.

The key objectives of the investigation on the single-cylinder research engine were to determine the impact of various engine operating parameters on the combustion performance and exhaust gas emissions and to evaluate the feasible operating range for a multicylinder application, particularly the required fraction of hydrogen or cracked ammonia. For the experimental investigation hydrogen was supplied by pressurized storage tanks. Due to the fact that the procurement and operation of the ammonia cracker is impacting the capital expenditure and the operating costs of the complete system. Therefore, the maximum hydrogen volume fraction was limited to 10 % for full load operating. Since the total mass flow rates for lower load operation is reduced compared to full load operation, a higher hydrogen fraction is feasible. Nonetheless, in order to maintain high system efficiency, the focus was on using the smallest amounts of hydrogen possible. In this set of experiments the engine was operated with a given indicated mean effective pressure (IMEP) and a single independent parameter was varied while the other parameters were maintained at a fixed value. The combustion phasing, expressed as crank angle where 50 % of the fuel energy has been released (CA50), was maintained at a fixed value by adjusting the ignition timing. The intake manifold temperature was also maintained at a fixed value, while the manifold pressure was adjusted to achieve the target excess air ratio (EAR). The pressure in the exhaust manifold was set individually according to the turbocharger main equation.

2.2 Experimental results

The results of hydrogen fraction variations at three different IMEP are summarized in Figure *5*. The feasible operating range differs significantly for the three load levels. While engine operation at 25.5 bar IMEP is feasible even without the addition of hydrogen, reduced load levels require continuously increasing hydrogen fractions.

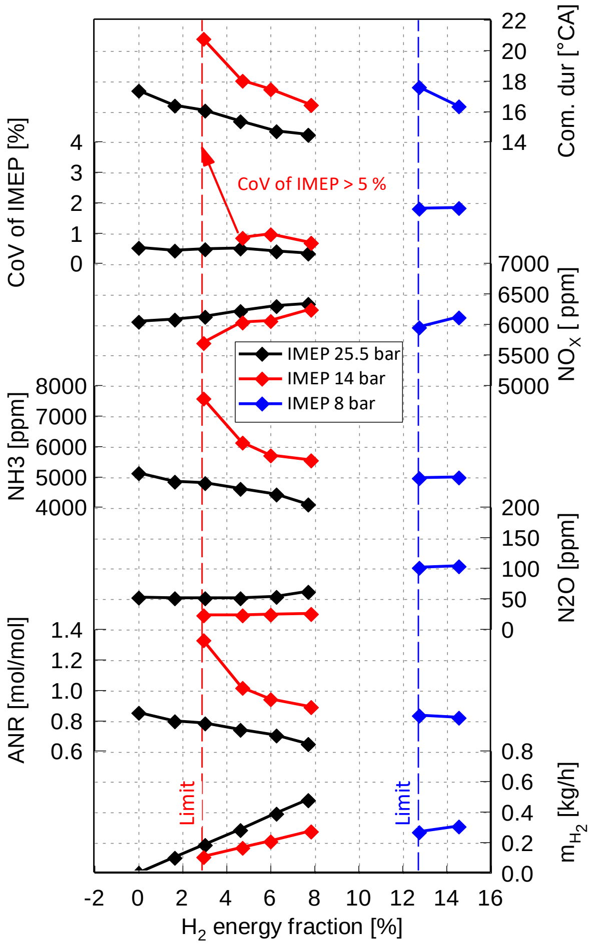

Figure 5: Performance and emissions results for hydrogen fraction variations at different load levels

Approaching the lowest feasible hydrogen fraction is characterized by increasing combustion duration, higher cyclic variability and higher concentrations of unburned ammonia in the exhaust gas. Therefore, even for high load operation, it might be desirable to operate the engine with small amounts of hydrogen.

2.3 Hydrogen flow rate requirements

The required hydrogen volume fractions in the engine can be translated into hydrogen mass flow rate requirements for the ammonia cracker based on the engine load, the total mass flow through the engine and engine efficiency. The expected range of required hydrogen mass flow rates is displayed in Figure *6* and shows that between the lowest and the highest demand a factor of approximately 8 needs to be covered by an ammonia cracker.

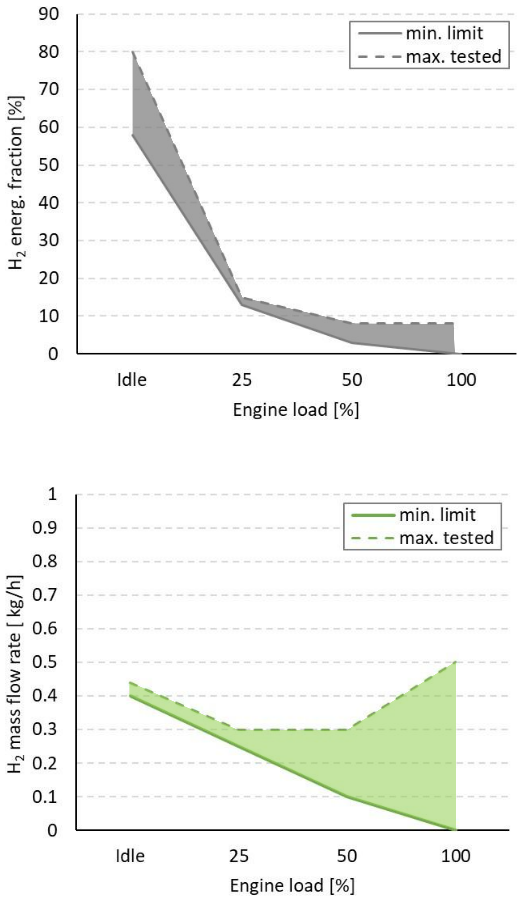

Figure 6: Required hydrogen fractions and hydrogen mass flow rates for the engine operating range

3 DEVELOPMENT OF AN AMMONIA CRACKER

A new technology concept is investigated that combines an electrically supported catalyst carrier with a catalytic partial oxidation reforming process. This concept aims for quick start-up capability, modular design, and high dynamic heating for ammonia reforming, enabling on-demand hydrogen production.

The dynamic operation is enabled by providing heat directly to the catalytic zone. This easy-to control option is based on electrically heated catalyst carriers on which the catalyst can be coated. The temperature at the catalyst can be increased by elevation of the electrical voltage applied. Another approach is autothermal operation mode (ATR), which combines both exothermic (2) and endothermic reforming reactions (1) on a single catalyst. In this mode a portion of the ammonia feedstock is utilized to generate the necessary heat for the reforming process. Ideally this operational method achieves a balance between the heat produced by the reaction and the heat needed for the endothermic reforming process.

To facilitate this operating mode air is introduced to the reaction system to supply the required oxygen. The oxygen ratio (λ – defined as the ratio of supplied oxygen to oxygen required for the complete combustion of ammonia, cf. Equation 3) is always maintained below 1.0. The more air is introduced, the higher the temperatures in the catalytic reactor. At the same time, the concentration of hydrogen in the product gas decreases, as larger volumes of water are produced from reaction (2) and the additional nitrogen volume increases with higher air flow rates. A balance solely based on reaction enthalpies would yield an oxygen ratio of approximately 0.13.

$$4NH_{3(g)} + 3\,O_{2(g)} \rightleftharpoons 2\,N_{2(g)} + 6\,H_2O_{(g)}$$

$$\Delta_R H = -\,316.8\ \text{kJ/mol}_{NH3} \quad (2)$$

$$\lambda = O_{2,\ \text{introduced}} \,/\, O_{2,\ \text{stoichiometric needed for total oxidation}} \quad (3)$$

$$NH_{3(g)} + \lambda^*(NH_{3(g)} + 3\,O_{2(g)} + 3 * 78 / 21\,N_{2(g)}) \rightleftharpoons$$

$$0.75\,H_{2(g)} + 0.25\,N_{2(g)} + \lambda^*(6\,H_2O_{(g)} + 3 * 78 / 21\,N_{2(g)})$$

$$\text{for } \lambda = 0.13\ \Delta_R H \text{ approx. } 0\ \text{kJ/mol}_{NH3} \quad (4)$$

A thermodynamic simulation of the reaction equilibrium in autothermal operating mode with varying amounts of air is presented in Figure 7 using the software CHEMCAD®. Heating up to the corresponding reaction temperature is taken into account, which implies that increasing the amount of air also increases the heat capacity of the gas stream because of its heat duty. The educts air and ammonia enter the simulated Gibbs reactor at 20 °C. Heat recovery from the product gas to the reactants as well as losses to the environment are not considered.

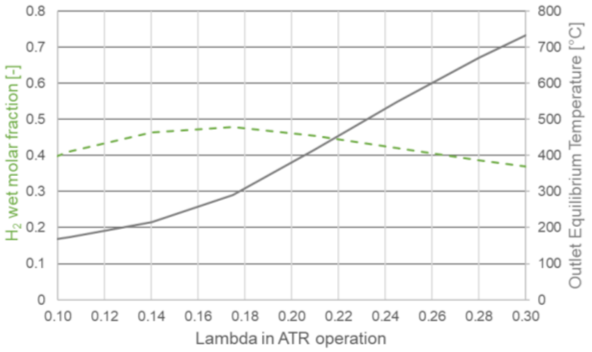

Figure 7: Results of thermodynamic simulation of autothermal ammonia reforming showing equilibrium temperatures and the hydrogen content based on the equilibrium composition.

The thermodynamic maximum fraction of hydrogen could be achieved at oxygen ratios of approximately 0.17 with corresponding outlet temperature of approximately 280 °C. At this temperature a literature review of catalysts shows a low activity for ammonia conversion and therefore the thermodynamic maximum is not reached. In the experimental section the temperature at the catalyst was increased by increasing the power input.

3.1 Cracker layout concepts

Electrically heated catalyst carriers, known from exhaust gas treatment, enable a particularly compact ammonia cracker design. They operate on the principle of resistive heating, converting electrical energy into heat based on ohmic resistance. These systems made of different steels are easy to control and can reach temperatures exceeding 600 °C in less than 10 seconds. They are long-term stable up to temperatures of 850 °C. Typical diameters for such systems range from 100 to 500 mm, and the electrical voltage typically applied ranges from 24 to 48 volts. Individual coatings with metallic catalyst materials are typically applied using dipping processes.

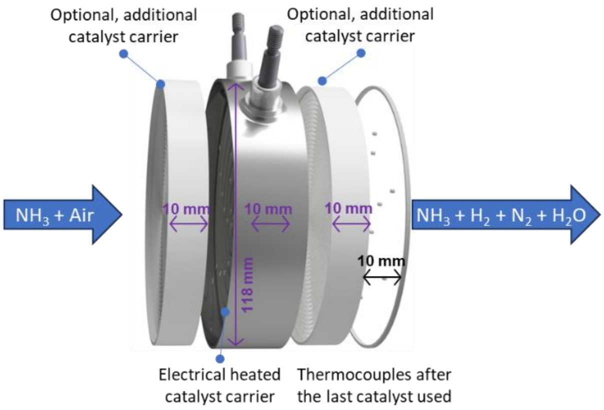

Figure 8: Cracker design based on an electrically heated catalyst carrier and additional catalyst carriers coated with a commercially available ruthenium washcoat

In the washcoat that ultimately adheres to the electrically heated catalyst carrier, highly dispersive metal components such as ruthenium are incorporated. Different Ru-washcoats are commercially available from various suppliers.

As can be seen in Figure 8 market-ready electrically heated catalyst carriers have a flat disk design and, in this embodiment, a maximum power of 2.4 kW. Leveraging serial designs that are produced in high volumes for the exhaust gas treatment of cars significantly reduces production costs, facilitating quicker commercialization. The disk used in the present experiments had a diameter of 118 mm, which is standard for heating up diesel oxidation catalysts and a height of 10 mm, therefore a volume of approximately 110 ml. In the following, this is referred to as the catalyst volume (V_{Cat}). To increase the reactive surface, the structure was extended by additional disks without electrical heating before and after the electrically heated catalyst carrier in some of the experiments, labelled as “optional, additional catalyst carriers” in Figure *8*. The distance between the catalyst carriers was approximately 8 mm. A computational fluid dynamic optimized mixer is used to distribute the incoming ammonia evenly across the catalytic zone.

The prototypes used in this work consisted of catalyst carriers welded together with a tube that has a cone upstream and downstream for gas inlet and outlet. A mixer was placed upstream of the inlet cone, and five K-type thermocouples with an accuracy of ±1.5 °C were placed in a circle at equal intervals ten millimeters downstream of the catalyst around the reactor circumference to evaluate the uniformity of temperature distribution and prevent overheating of the ruthenium-based catalyst. The average of the measurement values of those five thermocouples is indicated as the outlet temperature.

3.2 Experimental test setup

The cracker prototypes are connected to an experimental test setup with gas dosing, product gas analysis and safety equipment (Figure *9*).

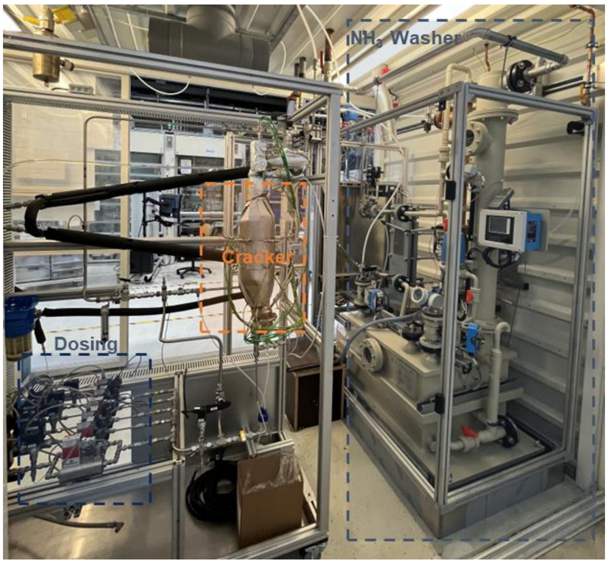

Figure 9: Experimental test setup including the dosing section with MFCs, the catalytic ammonia cracker and an ammonia washer.

The ammonia flow from a gas bottle with quality of 3.8 to the cracker prototype is controlled by mass flow controllers (MFC) that have an accuracy of ± 0.5 % of the measured value and ± 0.1 % of the final value. For all experiments in which no air was added to the gas stream supplied to the cracker, 10 vol% of argon was dosed to the total educt gas flow as an inert internal standard for analysis. The intake gas flow was maintained at room temperature.

Using a power supply, the electrical input power could be adjusted individually. The cracker was insulated with glass wool and sheet metal. The product gas is cooled by a counterflow water cooler. A regularly emptied condensate tank was installed to remove most of the water from the product gas flow. A partial flow of the product gas was passed through a gas chromatograph from the company Agilent 7890B type with thermal conductivity detector using a throttle valve. The developed chromatographic method allows for the analysis of hydrogen, ammonia, water, nitrogen and a mixture of oxygen and argon, which cannot be differentiated. Prior to entering the analyzer, water was condensed when using ATR, which produces water via reaction equation (2), to deliver comparable dry gas compositions. Furthermore, a mass spectrometer was connected to assess nitrogen oxide production when oxygen is present. In the literature [16] no unknown species that can represent nitrogen monoxide, nitrogen dioxide or nitrous oxide were detected and nitrogen production is dominant. The ammonia dissolved in the condensing water was not analyzed. It is assumed that the condensed water is saturated with ammonia for all operating points. Based on this assumption, it is ruled out that the dissolved ammonia has an influence on the overall product balance.

To purify the product gas before feeding the toxic gas into the exhaust system, a gas scrubber system from VUM was used to reduce the maximum residual ammonia content to below 20 ppm. The washing liquid was diluted sulfuric acid, whose pH-value and conductivity were continuously monitored. The unreacted ammonia was converted into a stable, less toxic, and non-corrosive ammonium sulfate solution. The maximum operating pressure of the washer was 80 mbar (gauge).

The cracker was operated in three different modes: thermal cracking with electrically heated catalyst carrier, autothermal reforming and a combination of both modes. The start-up procedure was based on switching on the electrically heated catalyst carrier before adding air for ATR operation. In ATR operation the electrical heater was shut down after the start-up procedure.

In the experimental measurements each operating point, characterized by the ammonia mass flow rate and the heat input, was maintained for at least 20 minutes. Initially, the ammonia volume flow rate was kept constant starting at 5 norm liters per minute while the electrical power input was incrementally increased. This adjustment was executed in electrical cracking mode through a stepwise increase of the electrical voltage, while in ATR, the power input was augmented by systematically elevating the air flow rate.

Both heat inputs can be described by the following equation, in which the first term applies to the electric input and the second term to the oxidation:

$$P_{tot} = P_{EL} + \lambda * \dot{M}_{NH3} * LHV_{NH3} \qquad (3)$$

The power input to the cracker was increased until one thermocouple at the cracker outlet indicated a temperature higher than 620 °C. A further increase of the power input would have increased the risk of damage of the catalytic material and was therefore avoided. Subsequently, the ammonia volume flow rate was increased, so that the outlet temperatures decreased again. As a result, the heat input could be successively increased again until one of the thermocouples at the cracker outlet indicated a temperature higher than 620 °C. Overall 228 operating points have been tested between 5 and a maximum of 44 norm liters per minute, which was limited by the maximum ammonia evaporation rate that could be supplied by the infrastructure.

4 RESULTS

Figure *10* and Figure *11* depict a selection of operating points that have generated the respective hydrogen mass flow rate with minimum heat input within the experimental series with the ammonia cracker. The red star markers show operating points with electrical power input, the green circles show operation points in autothermal operation mode.

The highest electrical power in the case of electrical heating that could be supplied without reaching 620 °C after the catalyst was 1.5 kW regardless of the ammonia mass flow rate. The maximum hydrogen production rate in this mode reached 0.125 kg/h. The highest power input via oxidation was 2.5 kW. The outlet temperatures in ATR with high hydrogen generation were significantly lower compared to electrical cracking.

The product gas contained only hydrogen, water, ammonia and nitrogen. No oxygen and nitrogen oxides were detected, which concludes that all oxygen introduced via air reacted to water through reaction (2). Oxidation reactions start catalytically at 230 °C. The oxygen ratios used were between

0.15 and 0.3, so 15 to 30 % of ammonia introduced was oxidized. The operating points depicted have oxygen ratios between 0.18 and 0.22 showing the favorable operation mode, suggesting that the resulting catalyst temperatures were too low at lower oxygen ratios and at higher oxygen ratios, too much ammonia was oxidized, resulting in less ammonia being available for reforming and hydrogen production.

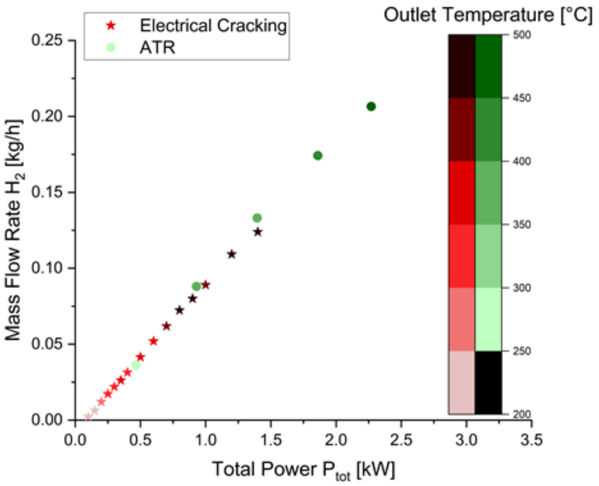

Figure 10: Average outlet temperatures and hydrogen production rates of selected ammonia cracking experiments as a function of heat input.

A linear relationship between the supplied power (P_{tot}) and hydrogen production can be observed. This relationship suggests that an increase in input power, whether through electrical or thermal heat sources, is directly correlated with an increase in hydrogen production. Adding catalyst volume has an influence on the GHSV based on the following equation with the educt gas volume flow at standard temperature and pressure:

$$GHSV = \dot{V}_{educts,\ STP} \ / \ V_{catalyst} \qquad (4)$$

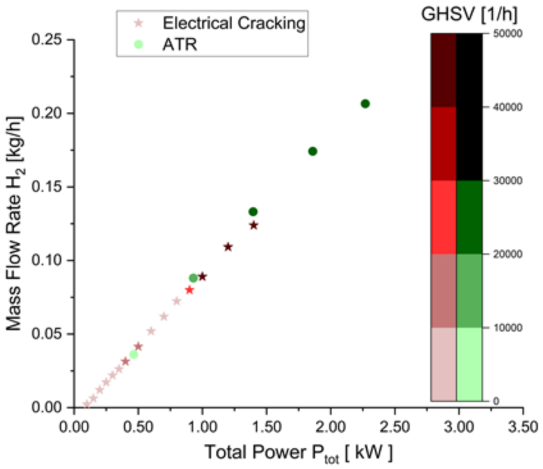

Figure 11: GHSV and hydrogen production rates of selected ammonia cracking experiments as a function of heat input.

The addition of air in ATR also influences the GHSV, as mainly oxygen and nitrogen are added to the educts. The maximum hydrogen mass flow rate within the series of experiments was 0.21 kg/h with the GHSV values of 30,000 1/h at ATR. Air was dosed with an oxygen ratio of 0.22 and an outlet temperature of 454 °C was reached. An overall ammonia conversion of 80.4 % was calculated, therefore 58.4 % of ammonia has been cracked and 22 % has been oxidized in this operating point. Accordingly, 19.6 % of the ammonia is passed through the cracker unconverted. This leads to the gas composition at the outlet of the ammonia cracker shown in Table 3.

Table 3: Volumetric gas composition at ammonia cracker inlet and outlet measured by gas chromatography at the maximum hydrogen production operating point

Composition ammonia cracker inlet [vol%]					
NH_3	N_2	Ar	O_2	H_2	H_2O
56.0	34.3	0.4	8.2	0	0
Composition ammonia cracker outlet [vol%]					
NH_3 measured	N_2 measured	Ar measured	O_2 measured	H_2 measured	H_2O calculated
8.1	41.9	0.3	0	36.1	13.6

If the ammonia cracker is applied to a multi-cylinder engine application, the power demand of the cracking process reduces the effective efficiency ($\eta_{e_{MCE}}$) of the complete system. In Figure 12 the impact of the H_2 energy fraction on $\eta_{e_{MCE}}$ is shown for three different cases. In the first case no cracker is used and H_2 is provided as a pure fuel source. In this scenario $\eta_{e_{MCE}}$, shows a marginal change in response to a variation in H_2 energy fraction and is mainly related to a change in gas properties and the combustion process. When ATR cracking is employed, a pronounced linear decrease in $\eta_{e_{MCE}}$ is observed compared to the case without cracker as the H_2 energy fraction is increased. A further decrease in $\eta_{e_{MCE}}$ can be seen by using electrical heating for the cracker. In this case it is assumed that the electrical power is supplied by the generator of the MCE. In this case, the efficiency chain (engine efficiency and generator efficiency) of the conversion of fuel into electrical power is taken into account and leads to a further decrease of $\eta_{e_{MCE}}$ compared to the ATR case.

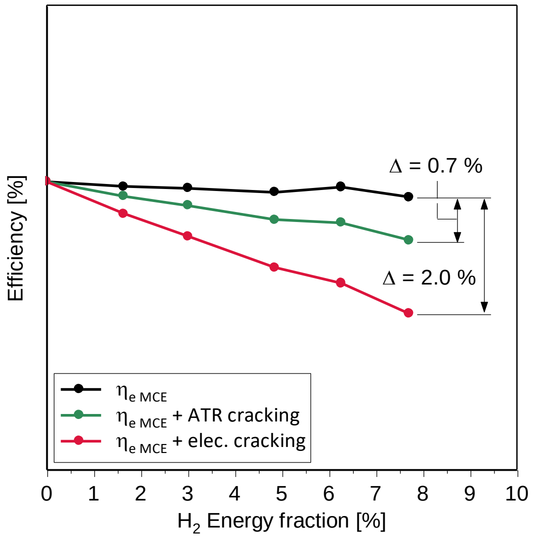

Figure 12: Impact of ammonia cracking on the engine effective efficiency as a function of the hydrogen energy fraction

5 CONCLUSIONS

The development of an ammonia cracker prototype that can be operated with electrically supported catalyst carrier and ATR based on partial ammonia oxidation presents a promising approach for on-demand hydrogen production in engines. The experiments conducted on a prototype ammonia cracker have demonstrated the effectiveness of ruthenium-based catalysts, expanding the knowledge from small-scale laboratory tests. The catalysts and their carriers used were stable for more than 150 hours of ammonia reforming operation.

The results exhibit the bifunctionality of ruthenium-based catalysts for both ammonia cracking and oxidation, initiating reactions at temperatures as low as 230 °C. This suggests that the light-off temperature of ammonia on ruthenium is near this temperature, but this must be investigated in more depth to define a reliable value. The catalysts were highly active for oxidation, as no residual oxygen was found in the product gas. Since no nitrogen oxides were detected either, all introduced oxygen can be accounted for in the water fraction of the product gas. A combination of electrical heating, which is advantageous for quickly achieving the desired temperatures at the start-up and ATR mode, which is advantageous for higher hydrogen production rates was successfully demonstrated. The highest hydrogen production rate was reached with an oxygen ratio of 0.22, which is slightly higher than the theoretical oxygen ratio of 0.17 for maximum hydrogen fraction (compare Figure *7*). This suggest that around 22 % of the heat input is released to the surrounding environment. This could be improved by insulation and direct integration to the engine.

The results have shown that a linear relationship between the supplied power and the produced hydrogen mass flow rate can be accomplished by selecting an appropriate set of operating conditions, i.e., heat supply to the catalyst, ammonia and air flow rates. Furthermore, based on this linearity, very simple process control and integration in the engine power control can be realized. The ammonia and air mass flow rates, however, will have to be controlled with a more complex scheme since no linear correlation was established for these quantities.

The comparison of outlet temperature values between cases with pure ATR operation and experiments with ATR and electrical heating suggests that the greater dilution with nitrogen in air has a significant impact lowering the outlet temperatures. The results emphasize the necessity of homogeneous heat input and uniform flow through the catalyst in the design of ammonia crackers to ensure optimal reaction conditions and improved efficiency. There is still more potential of hydrogen production with an electrically heated catalyst carrier, as only 1.5 of 2.4 kW could be used with one disk in the electrical cracking mode with the current design. Based on the results it is recommendable to use the pure electrical heating mode for start-up and afterwards switch to ATR by adding air if the electrically heated catalyst carrier is the costliest component of the cracker.

Compared to values from the literature high ammonia flows could be processed in a relatively small reaction volume, thus achieving high GHSV of 20,000 to 30,000 per hour and fast load changes. By extrapolation of the hydrogen production rate in ATR the required catalyst volume of a cracker that could supply 0.47 kg/h hydrogen for the SCE used in this experiment would be approximately 0.7 liters. This enables easy integration into the engine architecture later. Additional efficiency improvements might be achievable if engine exhaust gas enthalpy is used as a supplementary heat supply for the cracker. For combined heat and power engine applications where the engine heat streams are already utilized this option might not be available. A future, larger cracker setup that is coupled to the engine could benefit from enhanced insulation and reduced thermal bridges to the colder environment. This would result from a more favorable ratio of catalyst volume to external surface area, promoting better thermal efficiency and minimizing heat loss. Such design considerations are essential for optimizing the overall performance of the ammonia cracking system while leveraging waste heat from engine operations. Furthermore, the implementation of robust control strategies will be essential to optimize the operation of the cracker, balancing the heat supply and maximizing hydrogen production while minimizing potential risks associated with temperature fluctuations.

When considering the overall efficiency of the engine, the energy required for the cracking process must be taken into account. The additional energy required by the cracker, either from the ATR process or the electrical heating process, will reduce the overall efficiency of the engine. Estimations based on the laboratory experiments indicate that the reduction in engine efficiency is twice as high for the electrical cracking process as with the ATR process. The efficiency penalty due to the ammonia cracking process could potentially be reduced by an estimated 30 % through a reduction of heat losses to the environment.

In addition to the efficiency considerations the cracker operating strategies also have to be adjusted to the engine operating strategies and the engine combustion concept since different cracker operating modes result in different ratios of hydrogen and ammonia as well as nitrogen and water in the product gas. If the cracker product gas of ATR operation is fed into the pre-chamber of the engine the nitrogen dilution and presence of water might impact the ignition process in the pre-chamber.

6 DEFINITIONS, ACRONYMS, ABBREVIATIONS

ANR:	Ammonia to NO_X ratio
ATR:	Autothermal operation mode
BDC:	Bottom dead center
CA:	Crank angle
CA50:	Combustion phasing
CO_2:	Carbon dioxide
COV:	Coefficient of variation
GHSV:	Gas hourly space velocity
GWP:	Global warming potential
H_2:	Hydrogen
H_2O:	Water
IVC:	Intake valve closing
IMEP:	Indicated mean effective pressure
K:	Kelvin
kW:	Kilowatt
LHV:	Lower heating value
MCE:	Multi-cylinder engine
NH_3:	Ammonia
NO_X:	Nitrogen oxides
N_2:	Nitrogen
N_2O:	Nitrous oxide
P:	Power
RDS:	Rate determining step
Ru:	Ruthenium
SCE:	Single cylinder research engine
SI:	Spark ignition
STP:	Standard Temperature and Pressure
V_{Cat}:	Volume of coated catalyst carrier
λ:	Oxygen ratio

7 ACKNOWLEDGMENTS

The authors would like to acknowledge the financial support of the "COMET - Competence Centers for Excellent Technologies” Program of the Austrian Federal Ministry for Climate Action, Environment, Energy, Mobility, Innovation and Technology (BMK) and the Austrian Federal Ministry of Labor and Economy (BMAW) and the Provinces of Salzburg, Styria and Tyrol for the COMET Centre (K1) LEC GETS. The COMET Program is managed by the Austrian Research Promotion Agency (FFG).

8 REFERENCES AND BIBLIOGRAPHY

[1] Global Monitoring Laboratory, Trends in Atmospheric Carbon Dioxide, https://gml.noaa.gov/ccgg/trends/gl_gr.html, accessed: August 2023

[2] IPCC, 2022, *Climate Change 2022: Mitigation of Climate Change. Contribution of Working Group III to the Sixth Assessment Report of the Intergovernmental Panel on Climate Change [P.R. Shukla, J. Skea, R. Slade, A. Al Khourdajie, R. van Diemen, D. McCollum, M. Pathak, S. Some, P. Vyas, R. Fradera, M. Belkacemi, A. Hasija, G. Lisboa, S. Luz, J. Malley, (eds.)]*. Cambridge University Press, Cambridge, UK and New York, NY, USA. doi: 10.1017/9781009157926E

[3] IRENA and AEA. 2022. *Innovation Outlook: Renewable Ammonia*, International Renewable Energy Agency, Abu Dhabi, Ammonia Energy Association, Brooklyn

[4] A. Valera-Medina, F. Amer-Hatem, A. K. Azad, I. C. Dedoussi, M. de Joannon, R. X. Fernandes, P. Glarborg, H. Hashemi, X. He, S.

Mashruk, J. McGowan, C. Mounaïm-Rouselle, A. Ortiz-Prado, A. Ortiz-Valera, I. Rossetti, B. Shu, M. Yehia, H. Xiao, M. Costa, Energy & Fuels, DOI: 10.1021/acs.energyfuels.0c03685

[5] https://webbook.nist.gov/cgi/cbook.cgi?ID=C7664417&Mask=1

[6] Trangwachirachai, K., Rouwenhorst, K., Lefferts, L., Faria Albanese, J. 2024. Recent progress on ammonia cracking technologies for scalable hydrogen production, *Current Opinion in Green and Sustainable Chemistry*, Volume 49, DOI: 10.0945.

[7] Alboshmina, N. 2019. *Ammonia cracking with heat transfer improvement technology*. Doctoral thesis. Cardiff University, UK.

[8] Spatolisano, E., Pellegrini, L., de Angelis, A., Cattaneo, S., Roccardo, E. 2023. Ammonia as a carbon-free energy carrier: NH3 cracking to H_2, *Ind. Eng. Chem. Res*., Volume 62, doi: 10.1021/acs.iecr.3c01419

[9] Lucentini, I., Garcia, X., Vendrell, X., Llorca, J. 2021. Review of the Decomposition of Ammonia to Generate Hydrogen. *Ind. Eng. Chem. Res*. 60 (51), 18560–18611, DOI: 10.1021/acs.iecr.1c00843

[10] Fang, H., Liu, D., Luo, Y., Zhou, Y., Liang, S., Wang, X., Lin, B., Jiang L. 2022. Challenges and opportunities of Ru-based catalysts toward the synthesis and utilization of ammonia, *ACS Catal.*, 12 (2022), pp. 3938-3954

[11] Sun, S.; Jiang, Q.; Zhao, D.; Cao, T.; Sha, H.; Zhang, C.; Song, H.; Da, Z. 2022. Ammonia as hydrogen carrier: Advances in ammonia decomposition catalysts for promising hydrogen production. *Renewable Sustainable Energy Rev.* Volume 169, 112918, DOI: 10.1016/j.rser.2022.112918

[12] Wang, W.; Herreros, J. M.; Tsolakis, A.; York, A. P. E. 2013. Ammonia as hydrogen carrier for transportation; investigation of the ammonia exhaust gas fuel reforming. *Int. J. Hydrogen Energy*. Volume 38, 9907– 9917, DOI: 10.1016/j.ijhydene.2013.05.144

[13] Kim, J. H.; Um, D. H.; Kwon, O. C. 2012. Hydrogen production from burning and reforming of ammonia in a micro-reforming system. *Energy Convers. Manage.* 56, 184– 191, DOI: 10.1016/j.enconman.2011.12.005

[14] Plass, J., Tietz, C. Steffen, M. Engelmeier, L., Zinnemann, M., Nickig, N. 2024. Modellierung des dynamischen Betriebs einer Ammoniak-Crackeranlage für die Versorgung von Ammoniakmotoren unter Einbeziehung eines 2D-FVM-Reaktormodell, *AVL Simulation Conference*, Regensburg, Germany.

[15] Meléndez Rey, J., Antonio Medrano, J. 2024. Ammonia Cracking in membrane reactors for high purity hydrogen production, Ammonia Energy Association. https://ammoniaenergy.org/wp-content/uploads/2024/05/Ammonia-Project-Features-speaker-slides-May-2024.pdf

[16] Jang, J., Han, M. 2023. Ammonia autothermal reformer with air side-stream distribution for hydrogen production, international journal of hydrogen energy, Volume 49, pp. 1468-1481.

9 CONTACT

Univ.-Prof. Dr.-Ing. Nicole Wermuth
Institute of Thermodynamics and Sustainable Propulsion Systems, Research Area
“High Performance Large Engine Systems”
Inffeldgasse 19, 8010 Graz, Austria
Email: nicole.wermuth@ivt.tugraz.at
Phone: +43 316 873-30087